Available online at www.sciencedirect.com
SCIENCE DIRECT®
Atmospheric Environment 39 (2005) 39–50
ATMOSPHERIC ENVIRONMENT
www.elsevier.com/locate/atmosenv

Aerosol optical, chemical and physical properties at Gosan, Korea during Asian dust and pollution episodes in 2001

Sang-Woo Kim[a,b], Soon-Chang Yoon[a], Anne Jefferson[b,*], John A. Ogren[b], Ellsworth G. Dutton[b], Jae-Gwang Won[a], Young Sung Ghim[c], Byung-Il Lee[a], Jin-Seok Han[d]

[a]*School of Earth and Environmental Sciences, Seoul National University, Seoul, Korea*
[b]*NOAA Climate Monitoring and Diagnostics Laboratory, R/CMDL1, 325 Broadway, Boulder, CO 80305, USA*
[c]*Air Resource Research Center, Korea Institute of Science and Technology, Seoul, Korea*
[d]*Atmospheric Chemistry Division, National Institute of Environmental Research, Incheon, Korea*

Received 28 June 2004; accepted 24 September 2004

Abstract

In order to understand the influence of dust and anthropogenic pollution aerosols on regional climate in East Asia, we analyzed the aerosol optical, chemical and physical properties for two cases with high aerosol loading and assessed the radiative forcing of these cases. The 1st case study is a heavy dust episode (DE) in April (during ACE-Asia) 2001 and the 2nd case is a regional-scale pollution event in November 2001. The Ångström exponent (Å) for DE was 0.38 from sunphotometer measurements. The mean single scattering albedo (550 nm) at the surface reported during the pollution episode (PE, 0.88) was lower than that of DE (0.91). The concentrations of organic (OC) and elemental carbon (EC) measured during the PE were about 90% and 30% higher than DE. The aerosol mass scattering efficiency (α_s) of PE is a factor of about 2 higher than that of the DE. The difference in the mass absorption efficiency (α_a) of EC during DE and PE is small and within the measurement uncertainty. The diurnally averaged aerosol radiative forcing efficiency (ΔDFE, $W\,m^{-2}\,\tau^{-1}$) during DE is similar to results of other studies at Gosan.

Keywords: Asian dust and pollution; Light scattering; Light absorption; Aerosol radiative forcing; Gosan

1. Introduction

Eastern Asia is a major source region of combustion-related anthropogenic pollutants as well as wind-blown mineral dust aerosols. These aerosols have drawn much attention in recent years from the climate research groups in the context of the aerosol radiative effects (The Intergovernmental Panel on Climate Change (IPCC), 2001), because of their large but uncertain climate forcing. The regional climate effects of these aerosols are predicted to increase in the near future (Takemura et al., 2001).

According to results from the Asian Pacific Regional Aerosol Characterization Experiment (ACE-Asia) (Huebert et al., 2003), mineral dust aerosols had complex, highly varied chemical and optical properties (Anderson et al., 2003). Dust from East Asia was mixed with pollutants, creating a multi-component aerosol of great complexity and variability (Clark et al., 2004), causing a

*Corresponding author. Tel.: +1 303 497 6493
E-mail address: anne.jefferson@noaa.gov (A. Jefferson).

1352-2310/$ - see front matter © 2004 Elsevier Ltd. All rights reserved.
doi:10.1016/j.atmosenv.2004.09.056

significant perturbation to the radiation budget (e.g., Conant et al., 2003; Nakajima et al., 2003). The properties of pollution aerosols, not associated with dust, were poorly characterized during the ACE-Asia campaign. In order to better understand the influence of two aerosol types, dust and anthropogenic pollutant, on the regional climate environment in East Asia, we need to investigate the aerosol properties for both regional-scale pollution and dust storm cases. This study focuses on two case studies with high aerosol loading, where the 1st case study is a heavy dust episode (DE) in April 2001 (during ACE-Asia campaign) and the 2nd case is a regional-scale pollution event in November 2001. The objectives of these case studies are to characterize and compare the meteorological fields as well as the aerosol optical, chemical, and physical properties measured at Gosan, Korea during dust and pollution episodic periods and to investigate their radiative forcing.

2. Measurements

Aerosol characterization measurements were made at Gosan (33.29°N, 126.16°E, 72 m), Korea in the spring (April) and autumn (November) of 2001. A summary of the instrumentation used in this study is given in Table 1.

2.1. Aerosol optical properties

The aerosol scattering coefficients (σ_{sp}) were measured at three wavelengths (450, 550 and 700 nm) with a nephelometer (TSI model 3563), as a function of scattering angle (7–170°) and RH (50–95%) for aerosol particles, having diameters $< 10\,\mu m$. The aerosol absorption coefficients (σ_{ap}) were measured with a Radiance Research Particle Soot Absorption Photometer at 550 nm. The data were corrected for sample area, flow rate and non-idealities. Detailed descriptions of these instruments, their operation, associated uncertainties and variability appear in Delene and Ogren (2002).

A Carter–Scott sunphotometer (model SP02), mounted on a Sci-Tech solar tracker, made measurements of aerosol optical depth (τ) at 412, 500, 675 and 862 nm wavelengths. Calibration of the sunphotometer was performed at the NOAA CMDL facilities (39.99°N, 105.26°W, 1700 m) using a Langley plot approach before, during and after the field campaign. The reported accuracy of the spectral τ is approximately ± 0.02.

Table 1
Measurements made at Gosan that are related to this study

Institute	Instrument	Measured/derived properties	Episodic periods[a]	
			Dust	Pollution
(a) *Aerosol chemical and physical properties*				
KME	Various	$PM_{2.5}/PM_{10}$—mass, ionic comp. $PM_{2.5}$—EC and OC conc.	○	○
HKUST	Sampler	$PM_{2.5}$—mass, EC and OC conc.	X	○
UW	Sampler	$PM_{2.5}$—mass, EC and OC conc.	○	X
CMDL	CN counter	Condensation nuclei conc.	○	○
(b) *Aerosol optical properties*				
CMDL	Nephelometer	σ_{sp}, Å	○	○
CMDL	PSAP	σ_{ap}, ω	○	○
CMDL	Sunphotometer	τ, Å	○	○
SNU	MPL	σ_{ep}	○	○
(c) *Solar radiations*				
CMDL	Pyrheliometer	Direct irradiance	○	○
CMDL	Pyranometer	Diffuse irradiance	○	○
(d) *Gas phase concentrations*				
UMIST	Various	O_3, CO, NO_2, SO_2	○	X
KME	Various	O_3, CO, NO_2, SO_2	X	○
(e) *Meteorological parameters*				
KMA	Various	Surface T, RH, WS, WD	○	○
KMA	Radiosonde	Upper air T, RH, WS, WD	○	○

[a] ○: sample available, X: no sample available.

Vertical profiles of the aerosol extinction coefficient (σ_{ep}) were measured by a single-channel micropulse lidar (MPL; 523 nm). The vertical resolution was adjusted to 30 m, and the MPL was set to average and analyzed the backscattered signal every 10 min. Detailed descriptions of basic design and background of this instrument, its operation and σ_{ep} retrieval processes appear in Won et al. (2004).

2.2. Aerosol chemical and physical properties

Daily filter samples of $<2.5\,\mu m$ ($PM_{2.5}$) and $10\,\mu m$ (PM_{10}) particle diameter (D_p) were collected and analyzed for mass, elemental carbon (EC), organic carbon (OC) as well as major ionic compounds concentrations by three research groups:

(a) *Hong Kong University of Science and Technology (HKUST)*: Aerosols were collected on a 24-h schedule using a d-IAS sampler with a 2.5 μm cut size cyclone. OC and EC concentrations were measured using a thermal/optical carbon analyzer (Sunset Lab.). Complete descriptions are given in Yang et al. (2004).

(b) *University of Wisconsin-Madison (UW)*: Samples were collected each day for 24-h using a low volume sampler. Mass was measured at a temperature of 70 °C and RH of 35%. EC and OC were measured by the ACE-Asia EC/OC method based on NIOSH 5040, as detailed by Schauer et al. (2003).

(c) *Korea Ministry of Environment (KME)*: Daily filter samplings were conducted for the $PM_{2.5}$ and PM_{10} size fractions. The concentrations of OC, EC and ionic compounds were analyzed using a thermal/optical carbon analyzer (DRI, model 2001), ion chromatography (Dionex), atomic absorption spectroscopy (AAnalyst 800, Perkin-Elmer) and a UV spectrometer (Lamdar 20, Perkin-Elmer). Detailed descriptions of the instruments as well as the analytical methods and associated uncertainties appear in Ghim et al. (2003).

In addition, O_3, SO_2, NO_2 and CO measurements were made by the University of Manchester Institute of Science and Technology (UMIST) in April 2001 and by KME in November 2001.

2.3. Shortwave flux

The direct normal irradiance was measured by an Eppley normal incidence pyrheliometer and the diffuse irradiance was measured by an Eppley 8–48 black and white pyranometer, whose dome and receiver was shaded from the direct solar beam by a tracking disk in the short-wave regime (0.28–3.0 μm).

2.4. Meteorological parameters

Meteorological measurements, including temperature, relative humidity, wind speed (WS), and direction at the ground level were continuously measured at Gosan weather station, maintained by the Korea Meteorological Administration (KMA). Also, upper air radiosonde data of these quantities at the site were measured twice a day, on 00 and 12 UTC, respectively.

3. Results and discussions

3.1. Designation of Asian dust and pollution episodes

Fig. 1 shows variations of daily averages of the meteorological parameters and gas phase and particulate matter concentrations in April and November 2001.

According to the MPL observations, a large Asian dust storm swept over the Gosan site from 10 to 14 April, with a column Ångström exponent (Å) of 0.38. This dust event is easily recognized by an increase in the coarse particle mass concentrations, when the ratio of $PM_{2.5}$ to PM_{10} decreased to 0.57. These 4 days, when dust was the dominant aerosol, were designated as the "dust episode" (DE) in this study.

In November 2001, instead of a strong continental high-pressure system, a stagnant anti-cyclone overlay East Asia due to the atmospheric blocking by a low-pressure system over the Sea of Okhotsk. The same weather pattern repeated from 21 to 24 November and caused a build-up of pollutants in this region. In contrast to the DE these 4 days, when fine-mode pollutants were the dominant aerosol (ratio of $PM_{2.5}$ to PM_{10} of 0.89 and Å of 1.29), were designated as the "pollution episode" (PE) (Ghim et al., 2003).

We note that the dust particles were also mixed with pollution aerosols during DE (e.g., Huebert et al., 2003; Clark et al., 2004) and that local pollution aerosols also likely contribute to the aerosol high loadings during PE.

3.2. Meteorological conditions

The aerosol properties at Gosan were strongly influenced by meteorological conditions (Jefferson et al., 2004). The synoptic weather patterns during DE and PE were characterized by a fast moving cyclone system associated with a strong cold front and a stagnant anti-cyclone system, respectively. As shown in Fig. 1, the wind direction (WD) at the surface was north to southwest during the DE with a high WS ($\sim$13.1 m s^{-1}). During PE, WD was continuously from north to east with a relatively low WS ($\sim$7.5 m s^{-1}). For reference, the average WS for the last 30 years at Gosan has been 6.9 m s^{-1}.

Vertical profiles of WD and WS shown in Fig. 2 verify these characteristics. During DE, WD was from the north to southwest below 6 km, consistent with the results of the surface observations. During PE, the prevailing WD in the boundary layer was north to east.

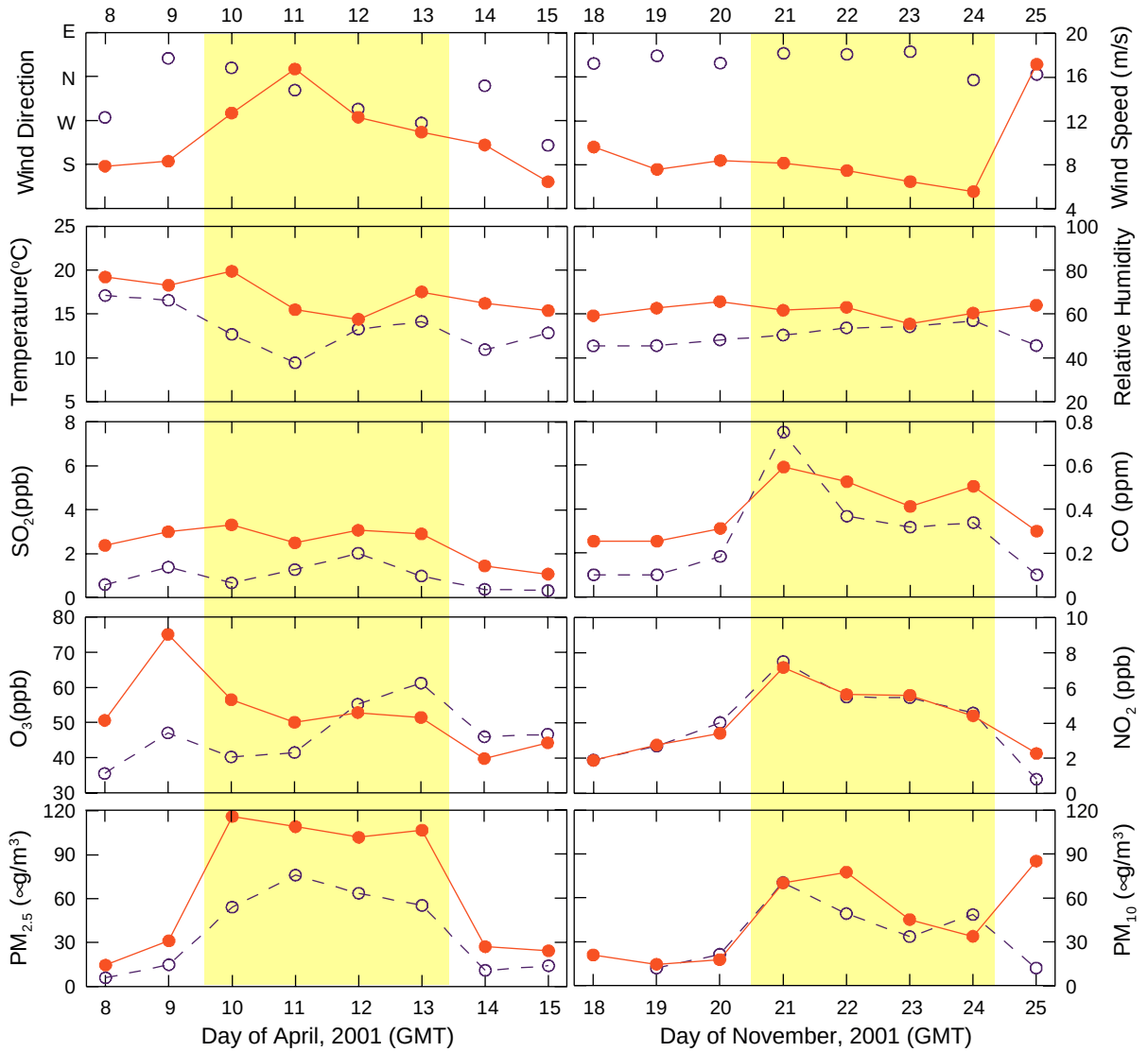

Fig. 1. Variations of daily averages of meteorological parameters, gas phase pollutant and $PM_{2.5/10}$ concentrations along with the designation of Asian dust and pollution episodes of April and November 2001, respectively. The shaded areas indicate dust and pollution episodes. The opened circles represent parameters in the left axis and closed circles, those in right axis.

WS increased with altitude for both the DE and PE cases, but the magnitude of WS during DE was higher than that during PE.

Fig. 3 shows the backward trajectories, calculated by NOAA HYSPLIT4 model (Draxler and Hess, 1998), at 500 and 1500 m altitudes at Gosan. The predominant airflow during DE, Figs. 2(a) and (c), consisted of north-westerlies and westerlies and its pathways between 500 and 1500 m altitudes were nearly identical. This dust storm generated in the deserts of inner China and passed over the industrialized coastal regions. During the PE, most of the air mass passed over industrialized regions of the east coast of China and the Korean Peninsula with relatively low WS under stable atmospheric conditions causing an accumulation of pollution aerosols.

3.3. Aerosol optical properties

The temporal evolution of the vertical distribution of aerosols is needed to better understand the surface and column aerosol properties. Fig. 4 shows the time–height indication (THI) plot of the aerosol extinction coefficient (σ_{ep}). During DE, three different patterns of the dust layer were observed. Before the frontal passage on 11 April, dust was in an elevated layer around 4 km, with

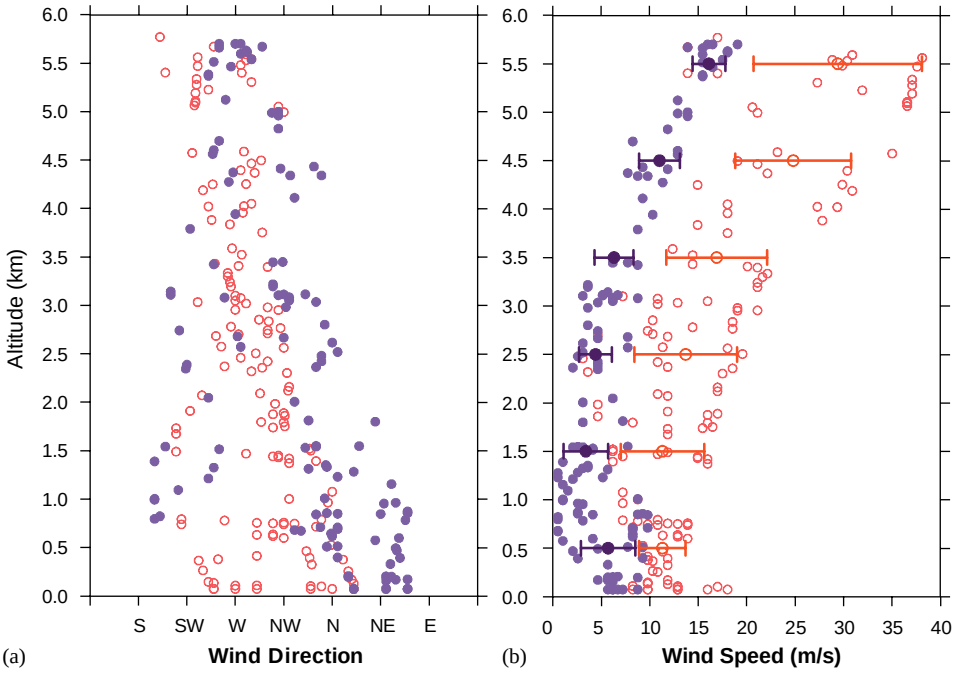

Fig. 2. Vertical profiles of (a) WD and (b) WS were taken from radiosonde measurements at twice a day, on 00 and 12 UTC during Asian dust (opened) and pollution (closed) periods. Symbols with error bars in (b) represent the average WS and its standard deviation for every kilometer.

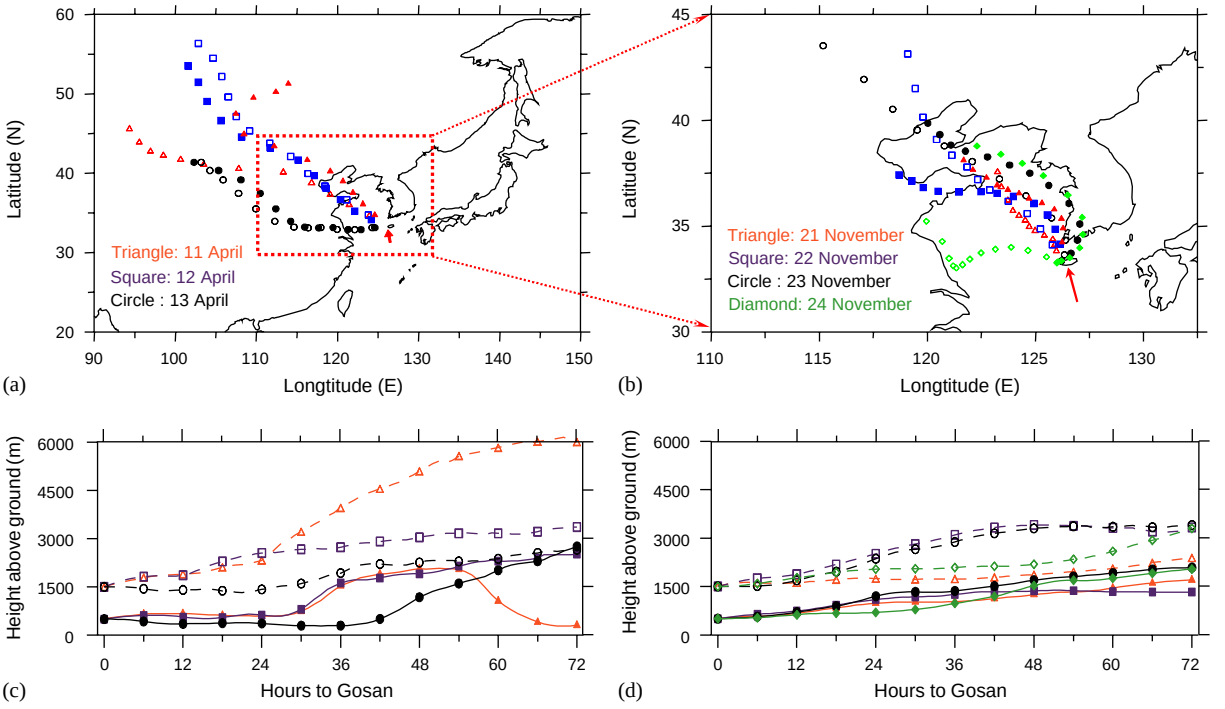

Fig. 3. Three days' backward trajectories at 500 m (closed) and 1500 m (opened) altitudes from Gosan during Asian dust (a and c) and pollution (b and d) episodes. The trajectory location was calculated at 6-h intervals: (a) and (b) on the horizontal plane, (c) and (d) on the vertical plane.

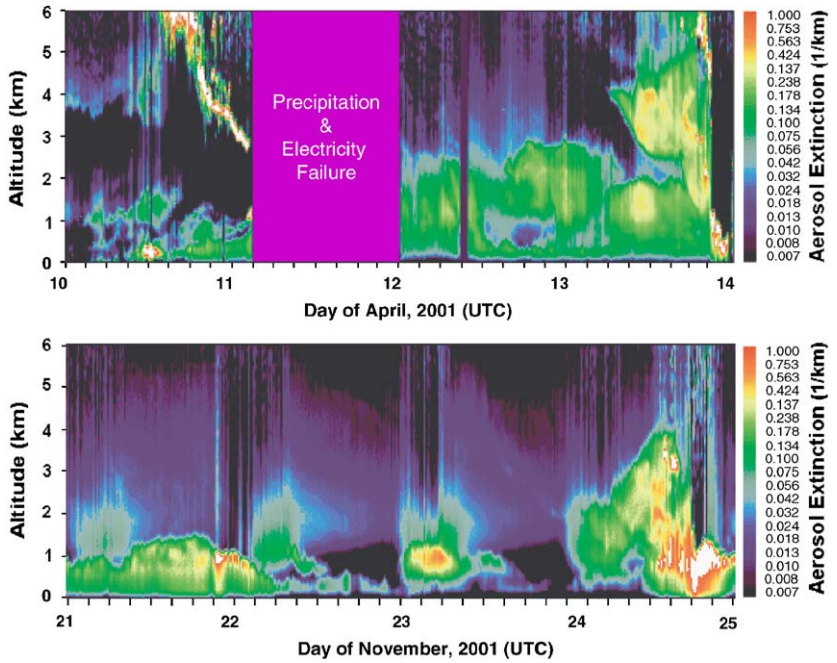

Fig. 4. Micropulse lidar measurements of aerosol extinction coefficient (523 nm) during Asian dust (top) and pollution (bottom) episodes at Gosan. The local time is UTC + 09 h.

Table 2
Comparison of means and standard deviations of aerosol optical properties measured by the in situ measurements during Asian dust and pollution episodic periods

Period	Parameters	CN (cm^{-3})	Extensive properties		Intensive properties	
			σ_{ap} ($M\,m^{-1}$, 550)	σ_{sp} ($M\,m^{-1}$, 550)	Å (450/700)	ω (550)
Dust	Mean	4833.6	22.8	239.8	0.66	0.912
	S.D.	2954.5	10.4	64.2	0.40	0.027
Pollution	Mean	3508.1	25.4	244.2	1.40	0.880
	S.D.	883.2	12.5	123.3	0.16	0.017

σ_{ep} of 0.15–0.2 km^{-1}, and after the frontal passage, dust was observed below 3 km. On the afternoon of 13 April, an isolated dust layer appeared near 4 km with σ_{ep} of about 0.5 km^{-1}. This layer gradually thickened and continued until 21 UTC on April 13, when it rained. The THI plot of σ_{ep} during the PE shows that the aerosol layer existed below 2 km from 21 November to 12 UTC on 22 November with $\sigma_{ep} < 0.2\,km^{-1}$. The maximum in the aerosol loading at 1 km was during the daytime, with σ_{ep} of 0.05–0.12 km^{-1}. On 24 November, an aerosol layer appeared below 3 km, followed by low-level clouds after 12 UTC.

Table 2 shows the means and standard deviations of the aerosol extensive and intensive properties during DE and PE. We performed a *T*-test to compare the means of the two groups. The variables in the shaded areas represent a significant difference. Particle number concentrations during DE were ~37% higher than that reported for PE. The means of σ_{sp} and σ_{ap} at 550 nm during PE were slightly higher than those of DE, but not statistically different. The mean single-scattering albedo (ω) at 550 nm reported during PE (0.88) was lower than that of DE (0.91) in a significance level of 0.05.

In spite of similar values of σ_{sp} at 550 nm, one distinguishing optical feature between the dust and pollution aerosols is the wavelength-dependent light scattering characteristics. Fig. 5 shows the wavelength dependence of the aerosol optical depth (τ) from the four-channel sunphotometer and σ_{sp} from a three-wavelength nephelometer. Å, negative of the slope of $\ln\tau$ (or σ_{sp}) versus $\ln\lambda$, from all wavelengths (λ) for DE (τ at 500 nm~0.618) was 0.38 and 0.61 from the sunphotometer and the nephelometer, respectively. Å for PE (τ at 500 nm~0.172) was roughly 2–3 times larger

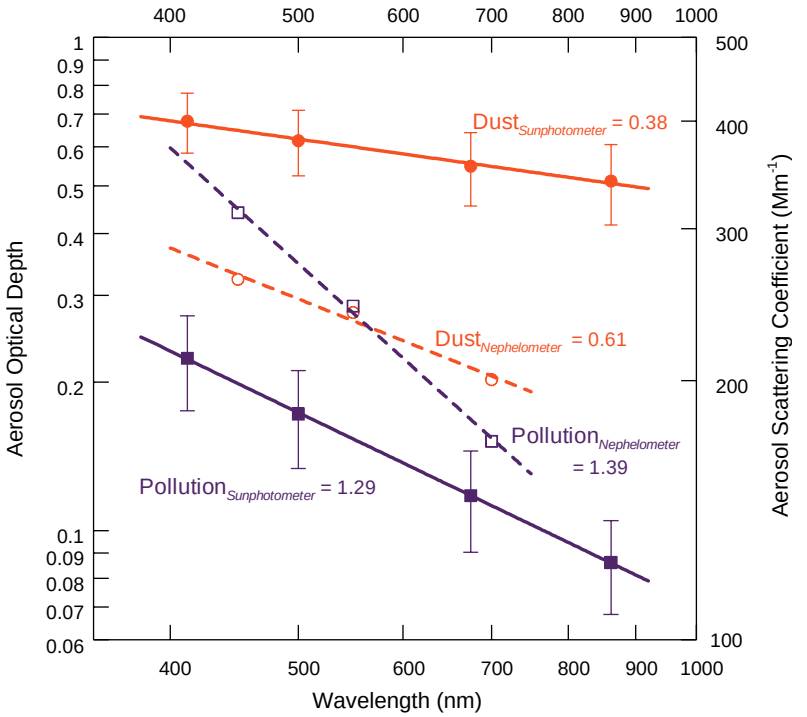

Fig. 5. The spectral variations of aerosol optical depth (τ; closed) from the sunphotometer and aerosol scattering coefficient (σ_{sp}; opened) from the nephelometer during the Asian dust (circle) and pollution (square) episodes. The standard deviation of τ is also plotted as error bars, but that of σ_{sp} is given in Table 2.

Table 3
Comparison of aerosol optical properties with those measured in worldwide locations

Location		σ_{ap}	σ_{sp}	ω	Sample duration (date/mon/yr)
Linan, China		23±14	353±202	0.93±0.04	28/10/1999–01/12/1999
Beijing, China		83±40	488±370	0.81±0.08	11/06/1999–16/06/1999
Yulin, China		6±10	160±196	0.95±0.05	31/03/2001–01/05/2001
Kaashidhoo, Maldives		16±9	73±28	0.82±0.03	15/02/1999–30/04/1999
Bondville, USA		5±2	57±18	0.92±0.03	19/09/1996–26/09/2000
Lamont, USA		3±1	47±17	0.95±0.03	06/04/1997–26/09/2000
Ship R/B	Dust	12±6	181±82	0.94±0.02	ACE-Asia campaign
	Pollution	7±4	64±30	0.94±0.03	(April, 2001)
Gosan, Korea		10±8	89±46	0.88±0.06	02/04/2001–28/02/2002
Aircraft C-130	Dust	9±2	135±23	0.95±0.02	ACE-Asia Campaign
	Pollution	9±5	55±34	0.88±0.03	(April, 2001)
This study	Dust	22±11	240±64	0.91±0.03	10/04/2001–13/04/2001
	Pollution	25±13	244±123	0.88±0.02	21/11/2001–24/11/2001

than those of DE, with values of 1.29 and 1.39 from sunphotometer and nephelometer measurements, respectively.

The aerosol optical properties in this study are compared with those at other clean or polluted areas in Table 3. σ_{sp} and σ_{ap} of this study are roughly a factor of 2–3 higher than those of the average year-round measurements at Gosan (Jefferson et al., 2004) and those from the NOAA research vessel *Ronald H. Brown* (Carrico et al., 2003) and aircraft C-130 (Anderson et al., 2003) during the ACE-Asia campaign. σ_{ap} is similar to values measured at Linan, China (rural, but affected by large city; Xu et al., 2002) and is more than a factor of 3 lower than the mean values from Beijing, China (polluted urban; Bergin et al., 2001). σ_{ap} of this study is roughly a factor of 4 higher than at the rural location

(Bondville, IL and Lamont, OK; Delene and Ogren, 2002) in the US and 1.5 times higher than the INDOEX results at Kaashidhoo (Andrews et al., 2001). Particularly, the mean σ_{ap} is 3 times higher than the values observed at Yulin, China, which is located near the dust source region (Xu et al., 2004). Similar to σ_{ap}, the mean σ_{sp} is also lower than that from Beijing and Linan, but higher than those from the other locations. Based on these measurements, the mean ω of the PE is similar to the year-round mean of ω at Gosan (0.88 ± 0.06, Jefferson et al., 2004), whereas the mean ω of DE is higher by 0.03. The value of ω during the DE is higher than the values at Beijing (0.81) and Kaashidhoo (0.82), but is lower than those at the other sites. From comparisons of σ_{ap} and ω between Yulin and Gosan, we deduce that large amounts of light-absorbing anthropogenic pollutants were added to the dust plume during transport. Namely, the reduction in ω as the air mass moves from the dust source region to Gosan is due to the addition of fine pollution particles to the mineral dust (Höller et al., 2003; Clark et al., 2004).

Fig. 6 shows the relationship between σ_{ep} and ω during DE and PE. Similar to other polluted regions, ω increased with increases in σ_{sp} or σ_{ep} during the PE (e.g. Andrews et al., 2001). However, ω decreased with an increase in σ_{ep} during the DE. Here, the data points in the afternoon on 11 April, given in the dashed circle, were not considered due to the aerosol scavenging by light rain (<0.4 mm). This result implies that as the total mass concentration of the dust particles increased, so did the light-absorbing aerosol concentration, most likely through coagulation of black carbon containing aerosol during long-range transport.

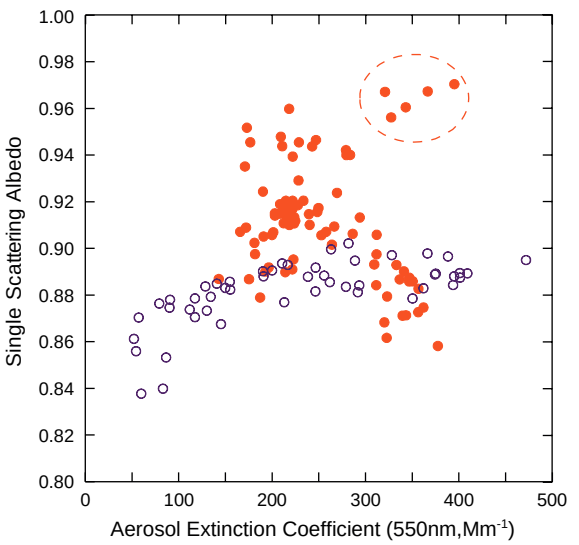

Fig. 6. Relationships between single scattering albedo and aerosol extinction coefficient during Asian dust (closed) and pollution (opened) episodes. Plots are based on all valid hourly averaged aerosol in situ measurements.

In general, the aerosol optical properties at Gosan during the DE and PE are more representative of prior measurements in urban rather than rural areas and are largely affected by light-absorbing aerosols, which can increase the aerosol forcing and forcing efficiency.

3.4. Aerosol chemical and physical properties

Integrated $PM_{2.5}$ and PM_{10} filter samples for mass, OC and EC, and major ionic concentrations during DE and PE are presented in Table 4. The majority of the aerosol mass during DE was in the coarse mode, as reflected in the 0.57 ratio of $PM_{2.5}$ to PM_{10}, whereas the aerosol was dominated by fine particles during PE, with a $PM_{2.5}$ to PM_{10} of 0.89.

For carbonaceous species, OC and EC concentrations measured during PE were about 90% and 30% higher than those of DE, respectively. Fig. 7 shows a comparison of OC and EC concentrations of this study with results from other studies at Gosan. The OC concentration for DE is within the range of previous results. However, the mean OC value during PE is nearly a factor of 2 greater than the other results (Kim et al., 2000). The EC concentrations are considerably higher than the results of other studies at Gosan. The source of high OC and EC concentrations during the PE are likely from the rice harvest and the burning of biomass after the harvest in China and Korea.

The mean ratios of OC and EC (OC/EC) are 2.7 and 3.8 for DE and PE, respectively. The greater value of PE is due to a larger increase of OC. These ratios of OC to EC are greater than the values from Seoul (<2; Kim et al., 1999), and are lower than the values from Beijing ($\sim$11.6; Bergin et al., 2001) and Linan ($\sim$11.0; Xu et al., 2002).

The increase in crustal elements (e.g. nss-calcium) was obvious during the DE. During the PE nss-sulfate, ammonium and nitrate, species that originated from anthropogenic sources rather than soil particles, formed 59% of $PM_{2.5}$ mass. During PE, the nss-potassium, which is a product of biomass burning, increased. These results compare well with those of Park et al. (2004) and Lee et al. (2001) at Gosan in Fig. 8. Park et al. (2004) analyzed 10 years of data from 1992 to 2002 for total suspended particles and Lee et al. (2001) studied $PM_{2.5}$ composition from 1996 to 1997. The concentrations of nss-sulfate, ammonium, and nitrate during the DE are similar to the above studies. However, those concentrations during PE were higher, by a factor of 2.2, 3.8 and 4.0 for $PM_{2.5}$, respectively. During DE only 42%, 70% and 21% of the sulfate, ammonium and nitrate were in particles smaller than $PM_{2.5}$ (J. Schauer, 2004, private communication). Most of the sulfate and nitrate resided in coarse mode particles.

Table 4
Comparison of PM_{10} and $PM_{2.5}$ mass, organic and elemental carbon, and major ionic aerosol concentrations during Asian dust and pollution periods (unit: $\mu g\,m^{-3}$)[a]

Species	Dust	Pollution	Measurement
PM_{10} mass	107.9±5.9	56.9±20.7	KME
$PM_{2.5}$ mass	62.3±10.1	50.4±15.2	KME
	66.5±20.1	N/A[b]	UW
	58.8±13.6	N/A	HKUST
$PM_{2.5}$ organic carbon	N/A	6.9±2.1	KME
	3.6±0.4	N/A	UW
	3.6±0.3	N/A	HKUST
$PM_{2.5}$ elemental carbon	N/A	1.8±0.8	KME
	1.4±0.5	N/A	UW
	1.3±0.4	N/A	HKUST
$PM_{2.5}$ ionic compounds			
nss-SO_4^{2-}	7.0 ± 2.2 (11.2)	15.9±5.4 (31.5)	
nss-Ca^{2+}	1.2±0.3 (1.9)	0.2±0.1 (0.4)	
nss-K^+	0.8±0.2 (1.3)	1.1±0.3 (2.2)	
NH_4^+	1.3±0.8 (2.1)	5.0±1.0 (9.9)	KME
NO_3^-	2.2±1.2 (3.5)	8.9±3.7 (17.7)	
Na^+	1.4±0.4 (2.2)	0.2±0.1 (0.4)	
Cl^-	0.8±1.1 (1.3)	0.3±0.1 (0.6)	
Mg^{2+}	0.3±0.0 (0.5)	0.1±0.0 (0.2)	

[a]The percentage of each ionic component relative to the $PM_{2.5}$ total mass of KME in parentheses.
[b]N/A: No sample available.

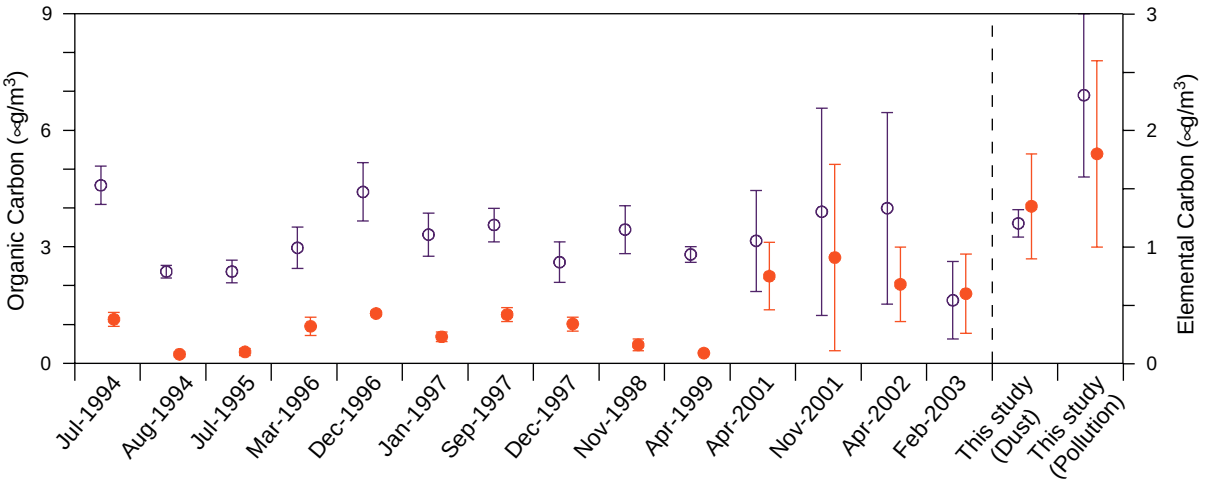

Fig. 7. Comparison of the organic (opened) and elemental carbon (closed) concentrations of this study with results from other studies at Gosan. The circle and bar represent mean and its standard deviation, respectively. Aerosol size cuts at all measurements were $PM_{2.5}$. The values from July 1994 to April 1999 are from Kim et al. (2000), April 2001; Yang et al. (2004), November 2001 to February 2003; Ghim et al. (2003) andGhim (2003).

3.5. Aerosol mass scattering and absorption efficiencies

The measurements of aerosol optical and chemical properties allow estimates of the aerosol mass scattering (α_s, $m^2\,g^{-1}$) and absorption efficiencies (α_a, $m^2\,g^{-1}$) shown in Table 5. α_s was estimated from the ratio of σ_{sp} ($D_p < 10\,\mu m$ and 550 nm) and PM_{10} mass concentration. α_s of the PE is a factor of 2 higher than that of DE. Lower α_s for dust may be due to the large particle size, non-spherical shape or lower refractive index of dust

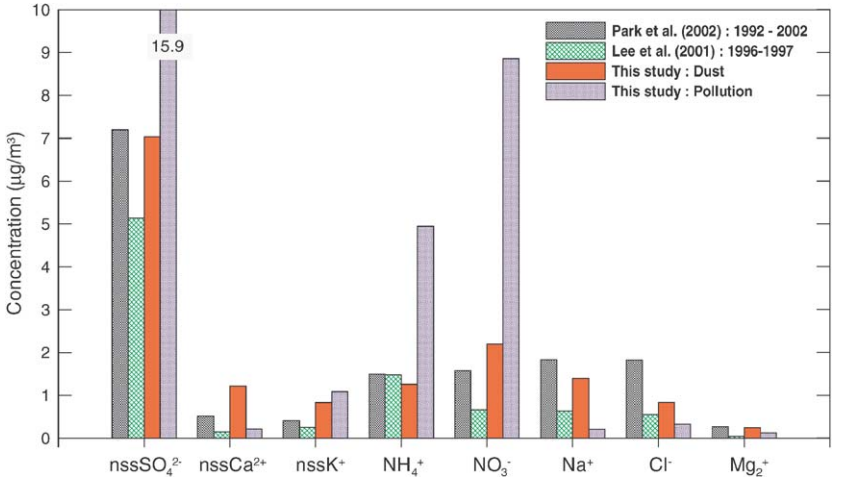

Fig. 8. Comparison of mean concentrations of the major ionic compounds of this study with results from other studies at Gosan.

Table 5
Comparison of aerosol mass scattering and absorption efficiencies during Asian dust and pollution periods (unit: $m^2 g^{-1}$)

Species	Dust	Pollution	Measurement
Scattering efficiency, α_s (PM_{10})	2.2 ± 0.1	4.5 ± 1.3	KME
Absorption efficiency, $\alpha_{a,}$ ($PM_{2.5}$)	N/A	13.8 ± 4.6	KME
	17.0 ± 1.5	N/A	UW
	16.9 ± 0.7	N/A	HKUST

compared to the pollution particles. Similar estimates of α_s have been founded in other studies for both urban and rural areas, 2.3–4.4 $m^2 g^{-1}$ (Bergin et al., 2001; Xu et al., 2002). α_s of PE is slightly higher than the upper end of this range.

α_a was estimated from the ratio of average σ_{ap} ($D_p < 10\,\mu m$ and 550 nm) and EC concentration from $PM_{2.5}$ measurements. For this estimate of α_a, we assume that the absorption and EC present in particles larger than 2.5 μm is negligible. The values of α_a for both DE and PE are larger than the range of values, 5–11 $m^2 g^{-1}$, reported for the US by Waggoner et al. (1981) as well as the values of $8.6 \pm 7.0\,m^2 g^{-1}$ in Linan (Xu et al., 2002). The sources of EC during DE and PE are likely from the burning of biomass associated with the harvest, emission of automobile exhaust and residential coal use. The contribution of mineral dust to σ_{ap} is expected to be small because the imaginary part of refractive index of the mineral dust particle is more than two orders of magnitude smaller than that of EC (Tegen et al., 1996). Thus, the α_a of the dust aerosol could be higher than the pollution aerosol due to the absorption of dust. However, α_a of DE falls within one standard deviation of that of PE and the difference between these values is not significant and could be due to the different EC measurement techniques.

3.6. Determination of aerosol radiative forcing

Based on this analysis of aerosol properties for high dust and pollutant loading episodes, we assess their relevance to the aerosol radiative forcing.

Clear-sky aerosol radiative forcing (ARF) in the short-wave regime (0.28–3.0 μm) is calculated by the hybrid method (Bush and Valero, 2003), which combines solar flux measurements under an aerosol-present atmosphere and model calculations for pristine atmosphere. Unlike the slope method, the advantage of the hybrid method is that it does not require measurements of the aerosol optical depth. Here, we use SBDART (Santa Barbara DISORT atmospheric radiative transfer; Ricchiazzi et al., 1998).

The diurnally averaged ARF (ΔDF, $W m^{-2}$) and forcing efficiency (ΔDFE, $W m^{-2} \tau^{-1}$) at the surface for the predominantly cloud-free days during DE and PE are given in Table 6. ΔDF is the averaged ΔF over 24-h calculated by the following two steps: all data are cloud-screened for clear sky, and then interpolated or

Table 6
Diurnally averaged aerosol radiative forcing at the surface and aerosol optical properties during Asian dust and pollution episodes

Period	(Day/Month)	Radiative forcing at the surface		Column properties		Surface properties						
		ΔDF ($W m^{-2}$)	ΔDFE ($W m^{-2} \tau_{500}^{-1}$)	τ_{500}	Å (412/675)	σ_{sp} ($M m^{-1}$)	σ_{ap} ($M m^{-1}$)	ω	OC ($\mu g m^{-3}$)	EC ($\mu g m^{-3}$)	α_s ($m^2 g^{-1}$)	α_a ($m^2 g^{-1}$)
Dust	12/04	−29.1	−77.5	0.375	0.672	243.8	28.8	0.90	3.8	1.0	3.8	17.4
	13/04	−56.5	−75.9	0.744	0.377	243.2	27.9	0.90	1.7	1.6	4.3	17.4
Pollution	21/11	−24.6	−86.9	0.283	1.308	264.8	40.8	0.89	9.9	3.0	4.9	13.7
	23/11	−16.4	−73.5	0.224	1.303	211.2	19.3	0.88	4.9	1.0	4.8	18.5
	24/11	−9.1	−76.0	0.120	1.350	211.0	13.7	0.87	6.4	1.8	4.3	9.4

extrapolated to fill in the missing periods. ΔDF is directly proportional to column aerosol amount, represented as τ. The largest ΔDF was estimated on the dust-dominated days, especially 13 April. However, ΔDFE, defined, as the ΔDF divided by the daily mean τ, depends on the aerosol upscatter fraction as well as the aerosol single scattering albedo. ΔDFEs during DE are expected to be lower than those of the mean PE values due to the weak absorption of dust particles (Tegen et al., 1996). However, ΔDFEs for DE are similar to those calculated for PE as well as the results of other studies at Gosan (Bush and Valero, 2003; Won et al., 2004) and suggest that either the dust is strongly absorbing or that a considerable amount of absorbing black carbon aerosol is associated with the dust. Variations in ΔDFEs with the surface single-scattering albedo or aerosol size (Å) are unclear. Day-to-day variations in the column water vapor may also affect the estimates of ΔDF and ΔDFE. The lower amount of water vapor observed by radiosonde on 23 and 24 November, compared to the other days may lead toward smaller estimates of surface ΔDF and ΔDFE.

4. Summary and conclusion

We analyzed measurement data for aerosol optical, chemical and physical properties at Gosan, Korea during heavy dust (DE, April 2001) and regional-scale pollution (PE, November 2001) episodes, and investigated their relevance for radiative forcing. The principle findings of our analysis are summarized below:

1. The meteorological fields were characterized by (a) long-range transport of dust by a fast moving cyclonic system associated with a strong cold front and short-range transportation by a stagnant anti-cyclonic system, and (b) northwesterly and north–northeasterly prevailing winds in the boundary layer for DE and PE, respectively.
2. The ratio of $PM_{2.5}$ to PM_{10} mass is 0.57 and 0.89 for DE and PE, respectively. Å values for the DE were 0.38 and 0.61 from the sunphotometer and the nephelometer, respectively. The single-scattering albedo reported during the PE (0.88) was lower than that of DE (0.91). However, the mineral dusts were also mixed with light-absorbing aerosols.
3. The OC and EC concentrations for the PE are ~90% and ~30% higher than those of the DE.
4. The increase in crustal elements (e.g., nss-calcium) was obvious during DE, whereas nss-sulfate, ammonium and nitrate dominated during the PE.
5. The aerosol mass scattering efficiency of PE is a factor of about 2 higher than those of DE. The difference in mass absorption efficiency of EC during DE and PE is small and within the instrument uncertainties.
6. The diurnally averaged aerosol radiative forcing efficiencies (ΔDFE) during DE and PE are similar and may reflect the association of light-absorbing aerosols with the dust.

The results of this study for high regional-scale dust and pollution aerosol loading conditions may be an indicator of future aerosol properties and emission levels if we assume that anthropogenic emissions and dust will continue to increase from China and all of East Asia.

Acknowledgements

We are grateful to the Gosan weather station staff, Dr. K. Bower (UMIST), Dr. J. Schauer (University of Wisconsin) and Dr. J. Z. Yu (HKUST) for providing data. This research was supported by the BK21 program and by the Climate Environment System Research Center and by the Korea Ministry of Environment as an Eco-technopia 21 project under grant 2001-44001-8. We thank the NOAA Office Global Programs for support of the CMDL measurements.

References

Anderson, T., et al., 2003. Variability of aerosol optical properties derived from in situ aircraft measurements during

ACE-Asia. Journal of Geophysical Research 108 (D23), 8647.

Andrews, E., et al., 2001. NOAA climate monitoring and diagnostics laboratory. Summ. Report 26, 60–79.

Bergin, M., et al., 2001. Aerosol radiative, physical, and chemical properties in Beijing during June 1999. Journal of Geophysical Research 106(D16), 17,969–17,980.

Bush, B.C., Valero, F.P.J., 2003. Aerosol radiative forcing at Gosan during the ACE-Asia Campaign. Journal of Geophysical Research 108 (D23), 8660.

Carrico, C.M., Kus, P., Rood, M.J., Quinn, P.K., Bates, T.S., 2003. Mixtures of pollution, dust, sea salt and volcanic aerosol during ACE-Asia: aerosol radiative properties as a function of relative humidity. Journal of Geophysical Research 108 (D23), 8650.

Clark, A., et al., 2004. Size distribution and mixture of dust and black carbon aerosol in Asian outflow: physiochemistry and optical properties. Journal of Geophysical Research 109, D15S09.

Conant, W., et al., 2003. A model for the radiative forcing during ACE-Asia derived from CIRPAS Twin Otter and R/V Ronald H. Brown data and comparison with observations. Journal Geophysical Research 108 (D23), 8661.

Delene, D.J., Ogren, J.A., 2002. Variability of aerosol optical properties at four North American surface monitoring sites. Journal of Atmospheric Science 59, 1135–1150.

Draxler, R.R., Hess, G.D., 1998. An overview of the HYSPLIT_4 modeling system for trajectories, dispersion, and deposition. Australian Meteorological Magazine 47, 295–308.

Ghim, Y., et al., 2003. Concentration variations of persistent organic pollutants in Gosan, Jeju during the polluted period in November 2001 and the yellow sand period in spring 2002 (in Korean). Journal of Korean Society of Atmospheric Enviornment 19, 469–490.

Höller, R., Ito, K., Tohno, S., kasahara, M., 2003. Wavelength-dependent aerosol single-scattering albedo: measurements and model calculations for a coastal site near the Sea of Japan during ACE-Asia. Journal of Geophysical Research 108 (D23), 8648.

Huebert, B.J., Bates, T., Russell, P.B., Shi, G., Kim, Y.J., Kawamura, K., Carmichael, G., Nakajima, T., 2003. An overview of ACE-Asia: strategies for quantifying the relationships between Asian aerosols and their climatic impacts. Journal of Geophysical Research 108 (D23), 8633.

IPCC (The Intergovernmental Panel on Climate Change), 2001. Climate Change 2001: The Scientific Basis. Cambridge University Press, Cambridge. 896pp.

Jefferson, A., Kim, S.-W., Kim, J., Ogren, J., Dutton, E., 2004. Source characterization of Asian aerosol at Gosan. South Korea. Proceedings of the International Radiation Symposium 2004, Busan, Korea, pp. 128.

Kim, Y.P., Moon, K.-C., Lee, J.H., Baik, N.J., 1999. Concentrations of carbonaceous species in particles at Seoul and Cheju in Korea. Atmospheric Environment 33, 2751–2758.

Kim, Y.P., Moon, K.-C., Lee, J.H., 2000. Organic and elemental carbon in fine particles at Kosan, Korea. Atmospheric Environment 34, 3309–3317.

Lee, J.H., Kim, Y.P., Moon, K.-C., Kim, H.-K., Lee, J.B., 2001. Fine particles measurement at two background sites in Korea between 1996 and 1997. Atmospheric Environment 35, 635–643.

Nakajima, T., et al., 2003. Significance of direct and indirect radiative forcings of aerosols in the East China Sea region. Journal of Geophysical Research 108 (D23), 8658.

Park, M.H., Kim, Y.P., Kang, C.H., 2004. Aerosol composition change between 1992 and 2002 at Gosan, Korea. Journal of Geophysical Research 109, D19S13.

Ricchiazzi, P., Yang, S., Gautier, C., Sowie, D., 1998. SBDART: a research and teaching software tool for plane-parallel radiative transfer in the Earth's atmosphere. Bulletin of the American Meteorological Society 79, 2102–2114.

Schauer et al., 2003. ACE-Asia intercomparison of a thermal-optical method for the determination of particle-phase organic and elemental carbon. Environmental Science and Technology 37, 993–1001, 10.1021/es020622f.

Takemura, T., Nakajima, T., Nozawa, T., Aoki, K., 2001. Simulation of future aerosol distribution, radiative forcing, and long-range transportation in East Asia. Journal of the Meteorological Socity of Japan 79, 1139–1155.

Tegen, I., Lacis, A.A., Fung, I., 1996. The influence on climate forcing of mineral aerosols from distributed soils. Nature 381, 681–683.

Waggoner, A.P., Weiss, R.E., Ahlquist, N.C., Covert, D.S., Will, S., Charlson, R.J., 1981. Optical characteristics of atmospheric aerosols. Atmospheric Environment 15, 1891–1909.

Won, J.-G., Yoon, S.-C., Kim, S.-W., Jefferson, A., Dutton, E.G., Holben, B., 2004. Estimation of direct radiative forcing of Asian dust aerosols with sun/sky radiometer and lidar measurement at Gosan, Korea. Journal of the Meteorological Society of Japan 82, 115–130.

Xu, J., Bergin, M.H., Yu, X., Liu, G., Zhao, J., Carrico, C.M., Baumann, K., 2002. Measurement of aerosol chemical, physical and radiative properties in the Yangtze delta region of China. Atmospheric Environment 36, 161–173.

Xu, J., et al., 2004. Aerosol chemical, physical, and radiative characteristics near a desert source region or northwest China during ACE-Asia. Journal of Geophysical Research 109, D19S03.

Yang, Xu, J., Wu, W.-S., Wan, C.H., Yu, J.Z., 2004. Chemical characterization of water-soluble organic aerosols at Juju Island collected during ACE-Asia. Environmental Chemistry 1, doi:10.1071/EN04006.